Imaging in children presenting with acute neurological deficit: stroke

Darshana D Rasalkar, Winnie C W Chu

Department of Imaging and Interventional Radiology, The Chinese University of Hong Kong, Prince of Wales Hospital, Shatin, New Territories, Hong Kong, China

Correspondence to
Professor Winnie C W Chu, Department of Imaging and Interventional Radiology, The Chinese University of Hong Kong, Prince of Wales Hospital, Ngan Shing Street, Shatin, New Territories, Hong Kong, China; winnie@med.cuhk.edu.hk

Received 6 April 2011
Accepted 10 March 2012
Published Online First 13 April 2012

ABSTRACT

Neurological deficits in the paediatric age group are much rarer than in adults; however, it is an urgent condition that relies heavily on imaging for a prompt accurate diagnosis. Neurological deficits caused by cerebrovascular diseases are defined as stroke, whereas conditions manifesting with neurological deficits without underlying cerebrovascular diseases are referred to as stroke mimics. To the best of the authors' knowledge, there is a lack of systematic pictorial review that collectively describes the imaging of neurological deficit in children. The purpose of the present series is to discuss the causes and imaging appearance of neurological deficits in childhood, based on the experience of a tertiary paediatric referral centre These are broadly categorised into stroke, infection, inflammation, metabolic disorder, cerebral neoplasms and drug poisoning. Different entities of stroke and their respective imaging findings are discussed. Paediatric stroke can further be divided into arterial ischaemic stroke, sino-venous stroke, haemorrhagic stroke and hypoxic–ischaemic encephalopathy.

Paediatric stroke is a relatively rare condition resulting in acute neurological deficits. The reported incidence of paediatric stroke is 2.1 to 13.1 per 100 000 children per year.[1–5] Nearly 50% of paediatric stroke are ischaemic in nature, while the other half are haemorrhagic or idiopathic in origin.[6] Another classification of paediatric stroke is based on the age of onset, divided into perinatal stroke (between 28 weeks of gestation and 28 weeks after birth) and childhood stroke.[7]

There is a significant overlap in clinical history, presentation and neurological examination in paediatric stroke despite various underlying causes. This often poses a diagnostic challenge[8] to physicians. Furthermore, clinical evaluation is often difficult in paediatric patients of very young age. Early identification of the stroke versus other causes of neurological deficit is crucial in guiding appropriate treatment, thus preventing lifelong debility and achieving a better prognosis.[9]

IMAGING CONSIDERATIONS IN PAEDIATRIC STROKE

Neurosonography is the preferred imaging modality for evaluating hypoxic brain injury in neonates.[10 11] The sensitivity of transcranial ultrasound is, however, low particularly in the first week of life and thus a negative study should not be interpreted as normal.[11–13] The sensitivity increases when transcranial ultrasound is performed after 7 days. The advantage of ultrasound, however, is that it can be performed at the bedside, which can minimise the risk of transportation or sedation. MRI remains the imaging of choice in highly suspected cases of stroke whenever the neonate can be transported to the radiology department. MRI has a higher sensitivity for the detection of white matter infarction and is capable of detecting underlying causes.[14] Diffusion-weighted imaging (DWI) enables the early detection of brain injury within hours after the hypoxic event,[15] and is useful in predicting the extent of infarct and outcome of deficit.[16 17] On magnetic resonance spectroscopy (MRS), stroke is characterised by reduced N-acetyl aspartate and increased lactate. The presence of a high lactate peak suggests a poor prognosis, with development of encephalomalacia in the affected region. For older infants and children with stroke, cranial MRI including magnetic resonance angiography (MRA) is considered the first imaging modality. Although catheter angiography is more sensitive in detecting medium and small vessel disease, it is only reserved for difficult cases in which endovascular surgical intervention is anticipated.[18]

CLASSIFICATION/CAUSES OF PAEDIATRIC STROKES

Arterial ischaemic stroke

The incidence of ischaemic stroke in childhood exceeds 3.3 per 100 000 a year.[5] The most common presentation of arterial ischaemic stroke (AIS) in childhood is hemiparesis attributable to the relatively frequent involvement of the middle cerebral artery (MCA). Other less common presenting features include altered mental status and focal neurological signs, such as aphasia and visual disturbance.[19] Stroke in the posterior circulation is rare and when it occurs it is usually associated with vertebral artery dissection,[20] presenting with ataxia, vertigo, or vomiting.[21] A focal pattern of infarction occurs in non-progressive arteriopathies and thromboembolic disease,[10] whereas a more diffuse pattern of infarction involving the deep watershed area is seen in the progressive occlusive vasculopathies. Braun *et al*[22] alternatively has classified AIS causes into arteriopathy (moyamoya, dissection, vasculitis, non-specific stenosis, systemic vasculitis with cerebral involvement or infarction after tentorial herniation); cardioembolic stroke (after congenital cardiac disease or cardiac surgery, after the exclusion of arteriopathy by vascular imaging); metabolic stroke accompanying metabolic diseases; and those with prothrombotic risk factors with or without associated arteriopathy. Out of these, moyamoya and metabolic stroke have been described in detail separately.

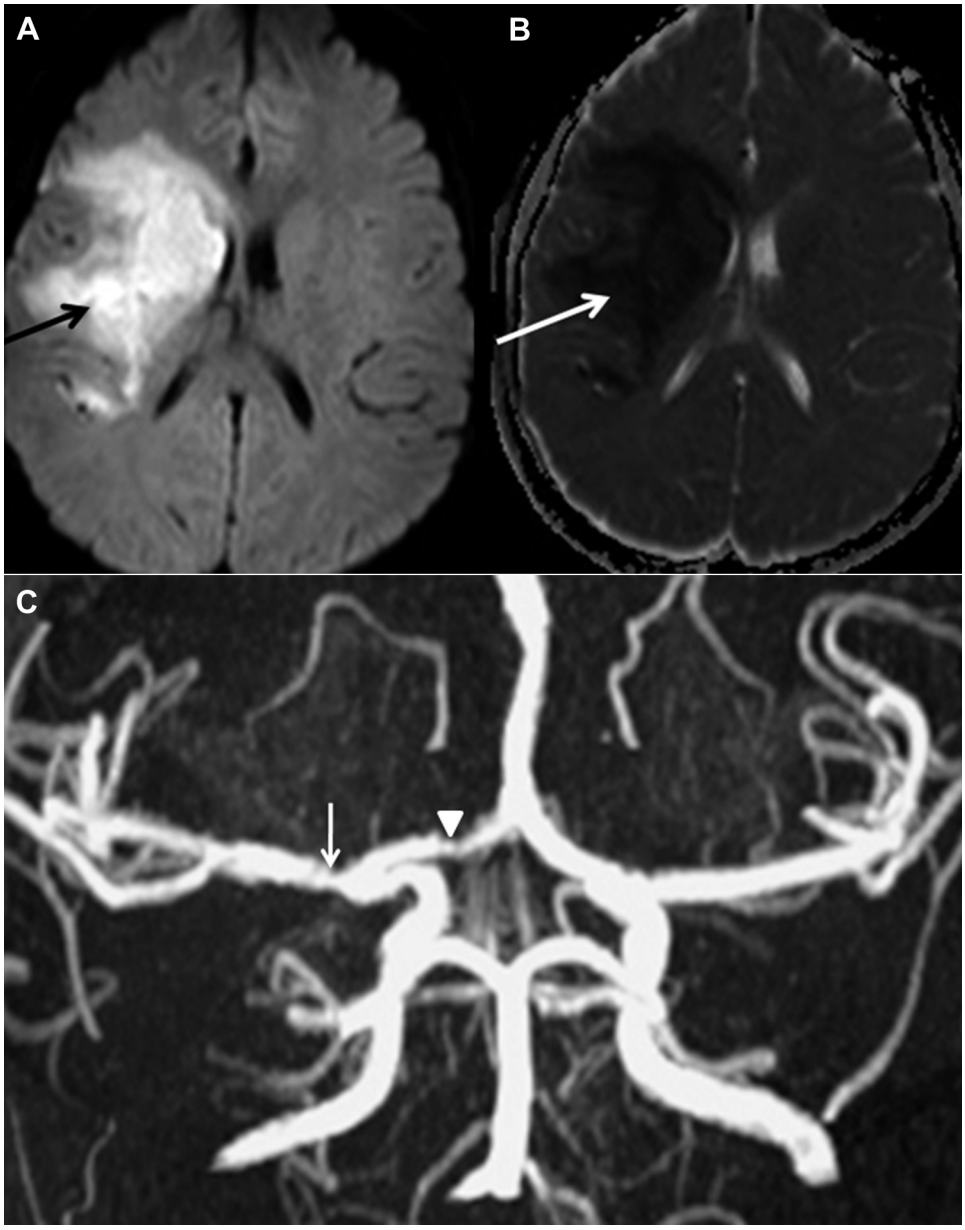

Figure 1 A 17-year-old patient presented with sudden onset of left-sided weakness and facial palsy. MRI brain: (A) diffusion-weighted imaging (DWI) and (B) apparent diffusion coefficient (ADC) map. Hyperintensity on DWI (black arrow) and corresponding hypointense signal on ADC map (white arrow) are compatible with restricted diffusion over the right parietal region. Features are suggestive of an acute infarct. (C) MRI angiogram of the circle of Willis using the time of flight technique reveals short segments of severe stenosis in the proximal M1 segment of the right middle cerebral artery (white arrow) and distal A1 segment of the right anterior cerebral artery (white arrowhead).

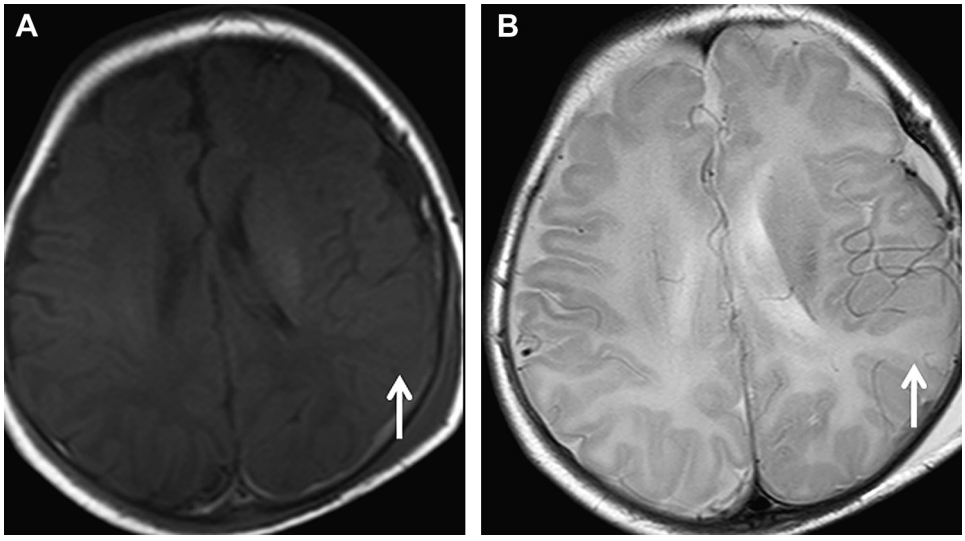

Figure 2 A 2-month-old boy was brought to an emergency department after observation of decreased left limb movement by the parents. MRI brain: (A) T1-weighted and (B) T2-weighted images. There is increased T2-weighted and decreased T1-weighted signal, which is nearly identical to the unmyelinated white matter, resulting in a 'missing cortex' appearance in the left parietal region (white arrows).

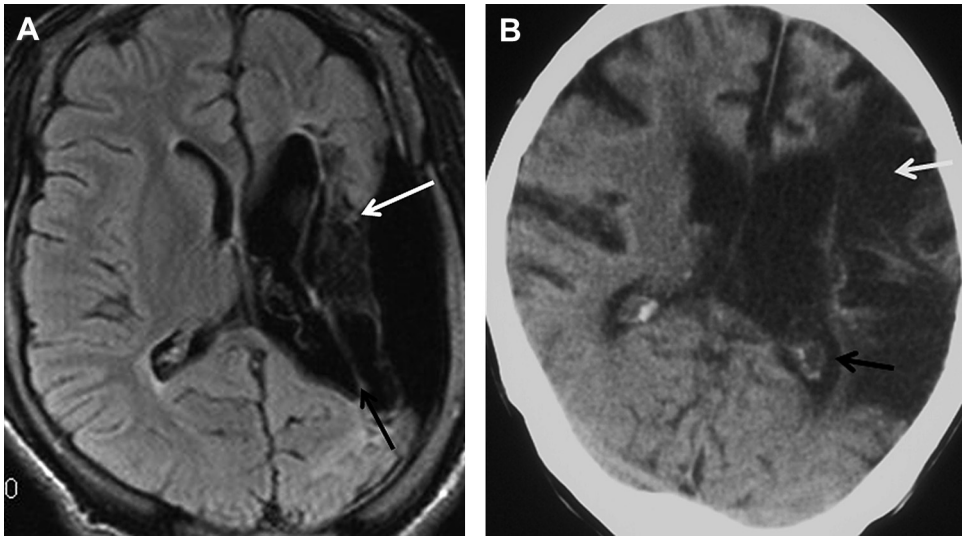

Figure 3 MRI and CT brain showing chronic/old left middle cerebral infarcts in two different adolescent patients with right hemiparesis since early childhood. The patient presented with a history of recent onset of seizures. (A) MRI, fluid-attenuated inversion recovery and (B) CT axial images showing cystic encephalomalacia in the left cerebral hemisphere involving the left frontoparietal lobe and left basal ganglia (white arrow). Note the ipsilateral cerebral atrophy and ex-vacuo dilatation of the left lateral ventricle (black arrow).

DWI is the mainstay of diagnosis in acute AIS. In practice, a high signal in DWI and low values on apparent diffusion coefficient (ADC) maps represent restricted diffusion due to cytotoxic oedema, which can be detected within minutes of onset allowing quick and reliable detection of ischaemic/infarcted areas (figure 1A,B). ADC maps usually normalise after approximately 5–7 days. Non-atherosclerotic cerebral arteriopathy constitutes a leading cause and is reported in up to 80% of children presenting with acute AIS;[4 20 21 23 24] the detection of which is important for secondary risk prevention. Time of flight (TOF) MRA is equally sensitive to conventional angiography for the detection of vasculopathy involving the internal carotid artery (ICA), proximal segments of the MCA and the anterior cerebral artery[25–27] (figure 1C). TOF–MRA might, however, overestimate the severity and length of a stenosis, whenever there is dephasing secondary to turbulence, slow flow or in-plane flow.[28] The above pitfalls can be overcome by contrast-enhanced MRA; however, the spatial resolution of MRA still limits an accurate assessment in medium and small-calibre intracranial arteries.[29 30]

In neonates with acute stroke, the ischaemic/oedematous cortex reveals an increased T2-weighted and decreased T1-weighted signal, which is nearly identical to the unmyelinated white matter, resulting in a 'missing cortex' appearance[10] (figure 2). The salvageable penumbra often reverses with an early thrombolysis or neurointerventions while the acute infarcted tissues probably evolve into a chronic infarct, resulting in cystic encephalomalacia, associated with brain volume loss and ex-vacuo dilatation of the ipsilateral ventricular system (figure 3).

Moyamoya disease/syndrome

Moyamoya disease is a progressive occlusive vasculopathy. On angiography, the characteristic appearance of dilated lenticulostriate perforating vessels is described as a puff of cigarette smoke or moyamoya in Japanese. Moyamoya can either be primary or

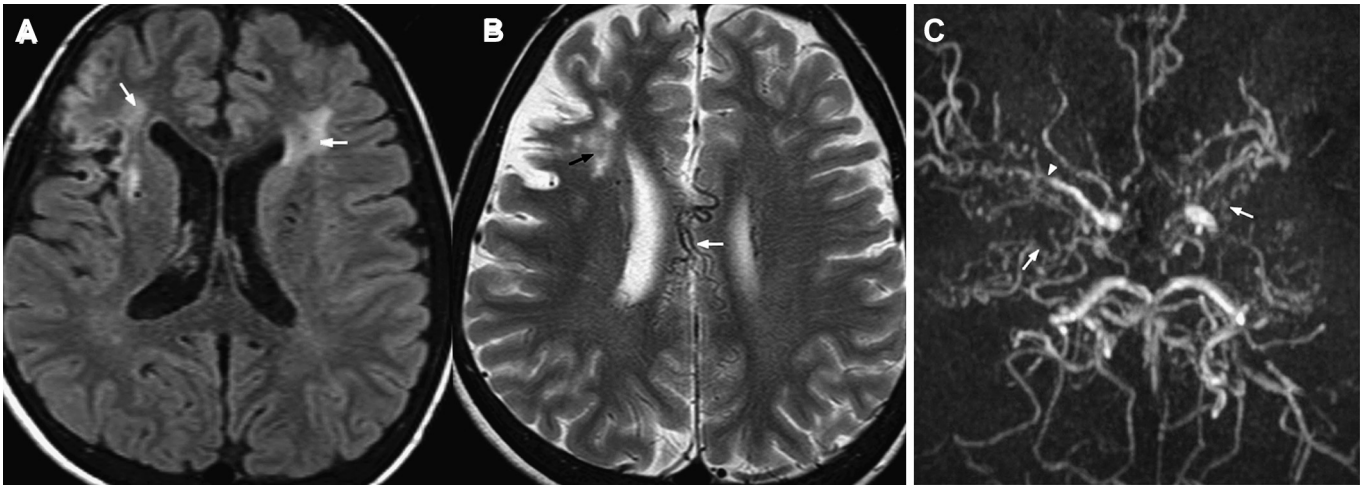

Figure 4 A 13-year-old boy presented with recurrent headache and repeated episodes of bilateral lower limb weakness. (A) Fluid-attenuated inversion recovery image shows hyperintensities in the bilateral frontal periventricular white matter (white arrows). (B) T2-weighted axial image shows prominent serpiginous collaterals in the parasagittal region (white arrow). (C) Magnetic resonance arteriography confirms absent bilateral internal carotid arteries associated and severe middle cerebral artery (MCA) stenosis (arrowhead). Note multiple serpiginous collaterals arising from the bilateral MCA (white arrows). Overall features are consistent with moyamoya disease.

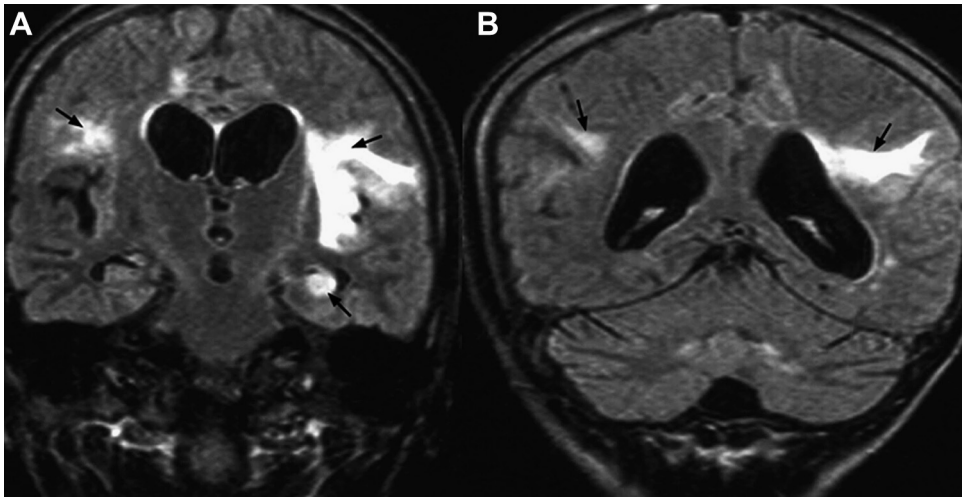

Figure 5 A 4-year-old girl presented with left-sided weakness. The cause of infarcts was not apparent at presentation but she was subsequently diagnosed to have mitochondrial myopathy, encephalopathy, lactic acidosi, and stroke syndrome by biochemical tests. No basal ganglia lesions were detected in this case. Cranial MRI (A and B). Fluid-attenuated inversion recovery coronal images show multiple T2 hyperintensities in the bilateral cerebral hemispheres involving the bilateral insular cortices, left hippocampus and bilateral corona radiata (black arrows).

idiopathic (in which case it is referred to as moyamoya disease), or secondary related to underlying disorders such as Down's syndrome, sickle cell disease, neurofibromatosis type 1 or cranial radiotherapy (in which it is referred to as moyamoya syndrome). The clinical symptoms include headaches, transient ischaemic attacks, AIS, intracranial haemorrhage or silent cerebral infarctions (figure 4A).[31] Initially, the steno-occlusive changes typically involve the distal intracranial ICA at the level of its bifurcation. Later, the stenosis progresses to involve the proximal anterior cerebral artery and MCA. Involvement of posterior circulation is rare, only occurring in the later stage and is reported in 25% of affected individuals.[32 33] The secondary collateral formation in response to the progressive stenosis and chronic cerebral hypoperfusion subsequently lead to multiple

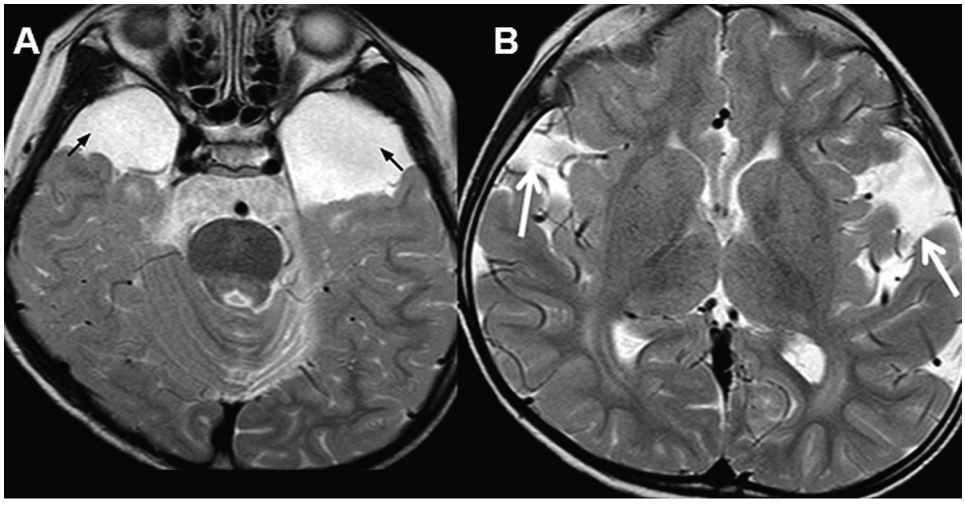

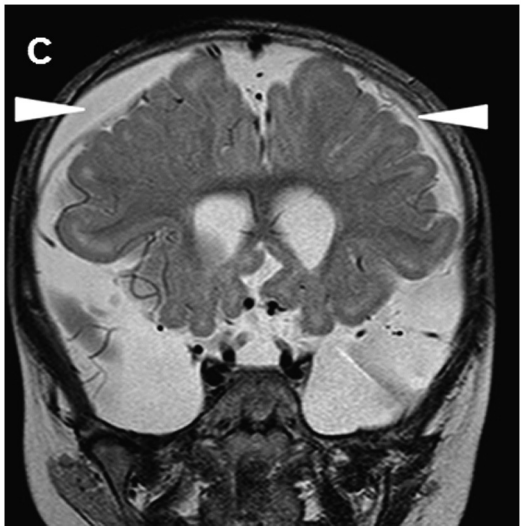

Figure 6 An 8-month-old girl was found to have rapidly increasing head circumference and gross developmental delay with repeated episodes of decreased left limb power and hypotonia. MRI scan of brain: (A, B and C) T2-weighted axial images show symmetric widening of the sylvian fissures (white arrows) with poor operculisation giving rise to 'bat wings appearance'. This is accompanied by an expansion of external cerebrospinal fluid spaces anterior to the temporal lobes (black arrows) resulting in frontotemporal volume loss. Chronic subdural collections (arrowheads) are present. Overall features are typical of 'glutaric aciduria type I'.

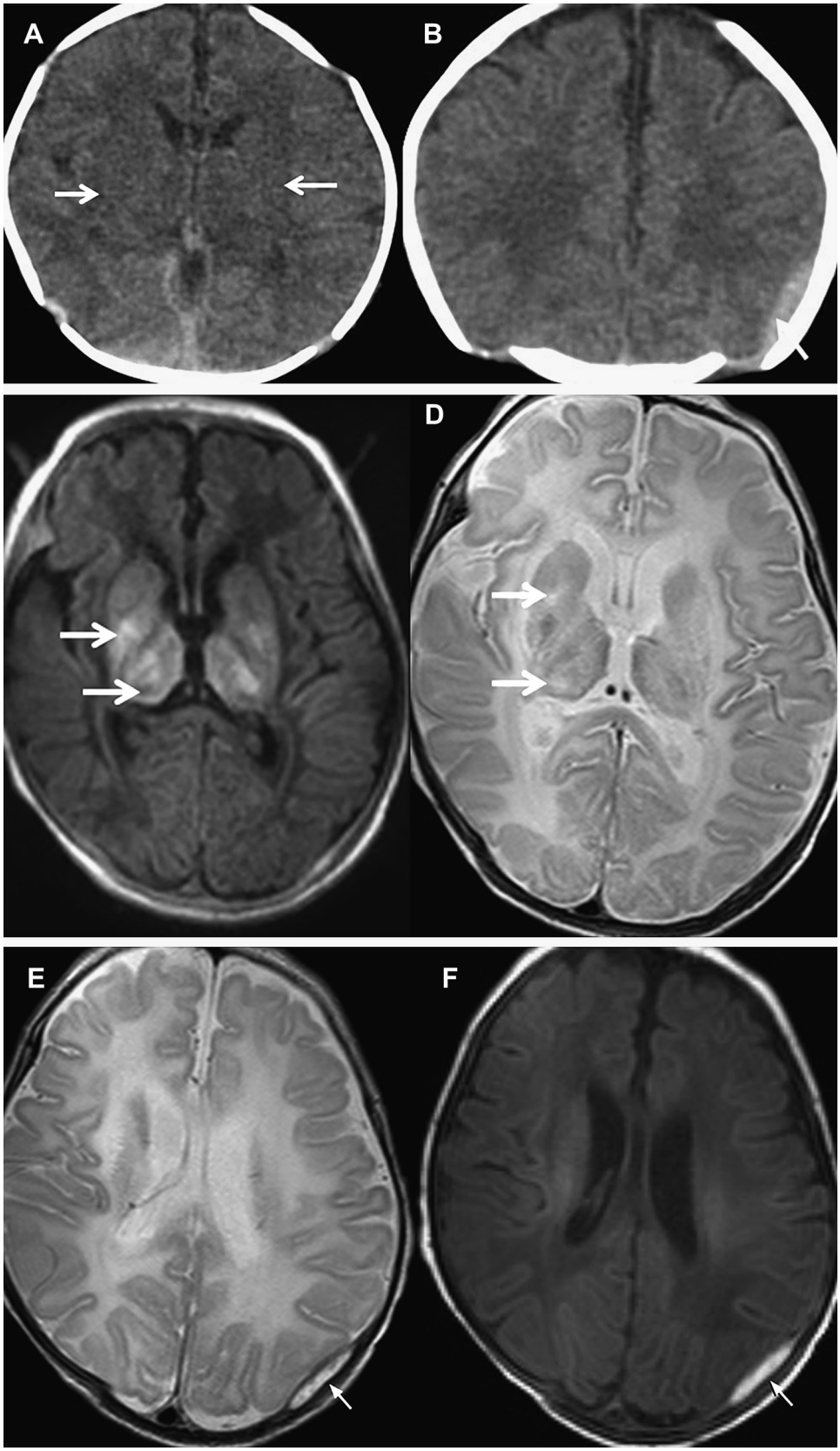

Figure 7 A preterm baby was born at home. She was found to have bradycardia, hypotonia and fixed pupils after 1 h of birth requiring active resuscitation for more than 45 min before arriving at the intensive care unit. Urgent CT brain (A) shows diffuse hypodensity in bilateral basal ganglia (arrows). This involvement of the deep nuclei is typically seen in of 'profound' hypoxia—ischaemia and (B) the presence of acute left posterior parietal epidural haematoma (arrow). (C) and (D) Follow-up MRI after 1 week shows T1-weighted hyper and T2 mixed signal intensities in the bilateral basal ganglia and thalami (white arrows) compatible with hypoxic—ischaemic brain injury. (E) T1-weighted and (F) T2-weighted axial MRI show T1-weighted hyper and T2-weighted hyperintense blood products compatible with the presence of methaemoglobin in subacute extradural haematoma (arrows).

dilated vascular channels, which often involve the lenticulostriate, thalamostriate perforators and the cortico-leptomeningeal vessels.[34] As these collaterals only have weak intimal walls intrinsically, they are prone to haemorrhage or small aneurysm formation.[35 36] Conventional MRI sequences demonstrate loss of flow voids of the terminal ICA and its proximal branches secondary to arterial stenosis. Dilated perforator vessels can be seen as flow voids within the basal ganglia, thalamus and basal cisterns on T2-weighted imaging (figure 4B). TOF—MRA (figure 4C) confirms the findings and together with structural imaging

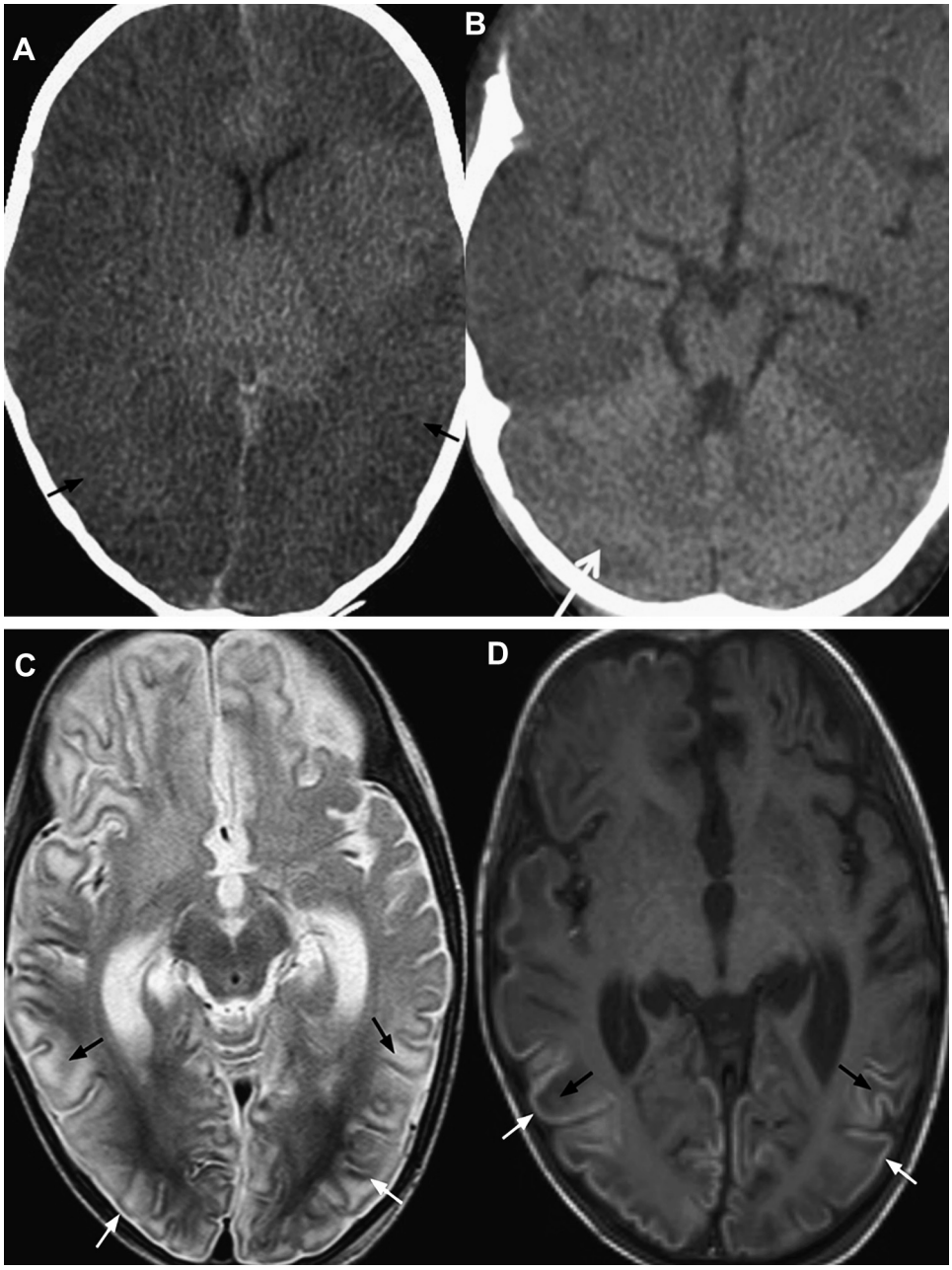

Figure 8 An 8-month-old girl was found to have acute onset stretching and tightness of all four limbs. On examination there was generalised hypertonia and hyperreflexia with decerebrate posture. (A) Emergency CT brain demonstrating profound loss of grey white matter differentiation bilaterally suggestive of global ischaemia (black arrows) with sparing of the cerebellum seen as reversal of cerebellum sign (white arrow) (B). Follow-up MRI after 3 months (C) T1-weighted and (D) T2-weighted images show T1-weighted hyperintense signal along the bilateral gyri (white arrow) and multiple T1-hypo and T2-hyperintense signal in the subcortical white matter; features suggestive of cortical laminar necrosis and established infarcts in the bilateral cerebral hemispheres.

has a sensitivity and specificity approaching 100%[37 38] for the diagnosis of moyamoya disease/syndrome.

Metabolic stroke

Inborn metabolic disorders are generally caused by spontaneous mutations or hereditary gene defects resulting in biochemical alterations involving one or more metabolic pathways. The clinical features are non-specific, variable and may at times mimic stroke.

A. Mitochondrial encephalopathy with lactic acidosis and stroke-like episodes

Patients with mitochondrial encephalopathy with lactic acidosis and stroke-like episodes (MELAS) syndrome are usually healthy at birth. Later, the affected children exhibit delayed growth, episodic vomiting, seizures, and recurrent cerebral injuries resembling stroke. These stroke-like events, probably as the result of proliferation of dysfunctional mitochondria in the smooth muscle cells of small arteries, may give rise to either permanent or reversible deficits. The disease course is progressive with periodic acute exacerbation.[39–41] Serum and cerebrospinal fluid lactate levels are usually elevated. MRI demonstrates multiple cortical and subcortical infarct-like lesions that cross vascular boundaries (figure 5), along with varying degrees of generalised cerebral and cerebellar atrophy. The parietal and occipital lobes and the basal ganglia are frequently involved. Follow-up MRI may show resolution and then subsequent reappearance of the abnormal areas. MRS may reveal the presence of lactate even when the conventional MRI findings are unremarkable. MRS can be regarded as a screening tool in patients with suspected mitochondrial cytopathy.[42]

B. Glutaric acidurea

Glutaric aciduria is a genetic disorder in which mutations in certain genes cause a deficiency or reduce the efficiency of

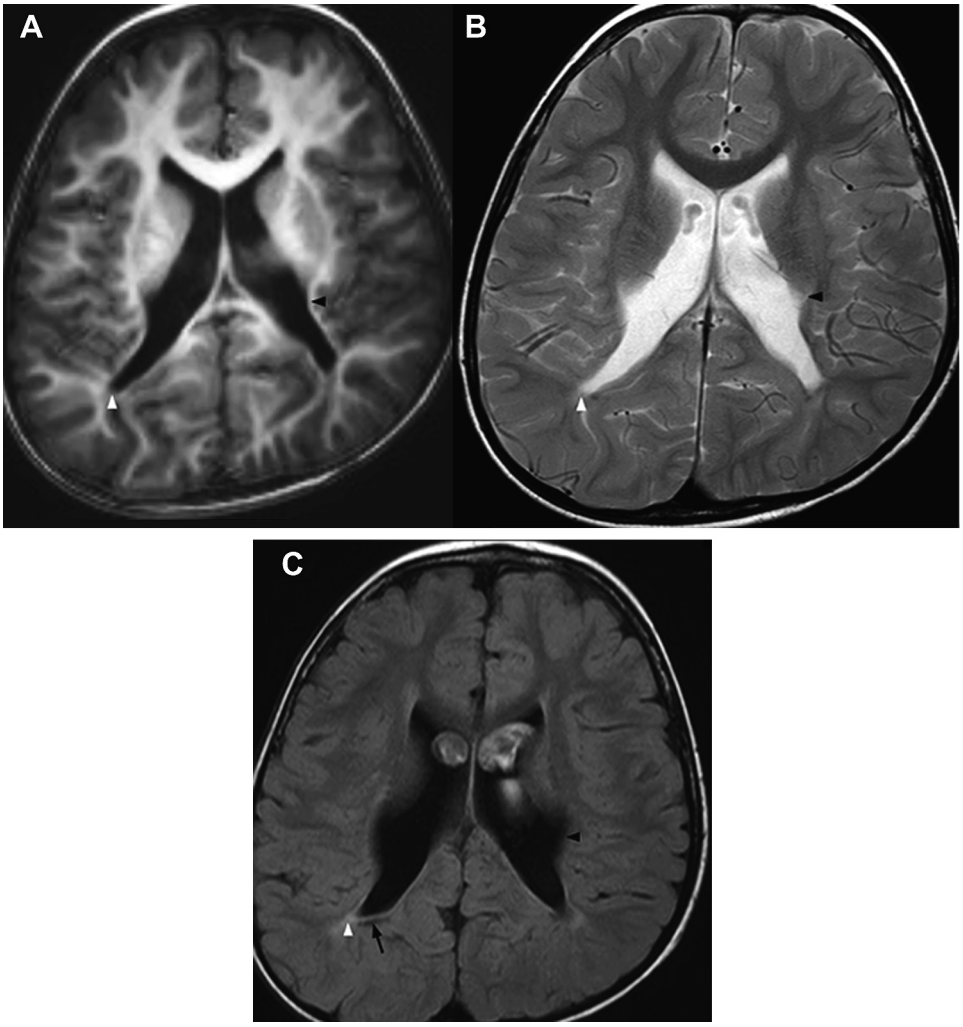

Figure 9 A 3-year-old boy with developmental delay and spastic diplegia. He was an ex-preterm baby delivered at 29 weeks of gestation with a history of asphyxia at birth. MRI brain: (A) T1-weighted; (B) T2-weighted and (C) fluid-attenuated inversion recovery (FLAIR) axial images showing T1-weighted iso to hypo and T2 hyperintensities in the bilateral periventricular white matter (white arrowhead) and ventricular enlargement (black arrowhead). Note there are cystic changes in bilateral trigonal regions, best appreciated in FLAIR images (black arrow). Features are suggestive of 'white matter injury of prematurity', a pattern of established hypoxic–ischaemic encephalopathy, typically seen in preterm injury.

mitochondrial enzymes. The majority of untreated children present with an acute stroke-like neurological crisis when the introduction of a high protein diet starts at approximately 6–18 months of age. Classically these children present with spasms, jerking, rigidity, weakness and a tendency for seizures with loss of sucking and swallow reflexes. Abnormal bleeding commonly occurs and may raise the suspicion of non-accidental injury due to the presence of subdural haematoma (SDH). However, there are characteristic neuroimaging features on MRI, which help to suggest the correct diagnosis (figure 6).[43] Elevated glutaric acid levels in either blood or urine are diagnostic. The mainstay of treatment is dietary manipulation aimed at reducing the production of glutaric acid and other intermediate metabolites by diet modifications.

Hypoxic–ischaemic brain injury

Hypoxic–ischaemic brain injury (HIE) is more common in preterm neonates than in term neonates.[11] Overall,

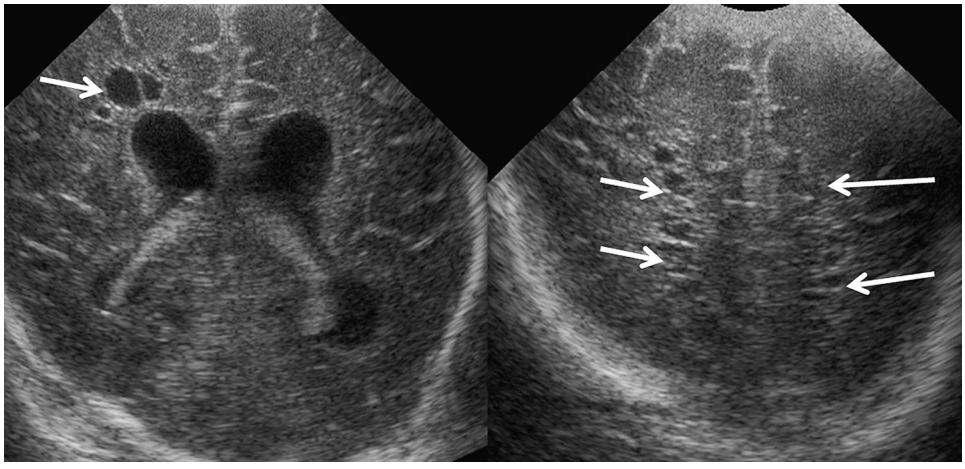

Figure 10 Ultrasound appearance of periventricular leucomalacia in a premature (32 weeks) twin male baby who presented with respiratory distress and hypotonia at birth. Note the multiple cysts occupying the frontal, parietal and occipital horn of the cerebral hemisphere (white arrows). They are not communicating with the ventricular system. Feature is suggestive of cystic encephalomalacia.

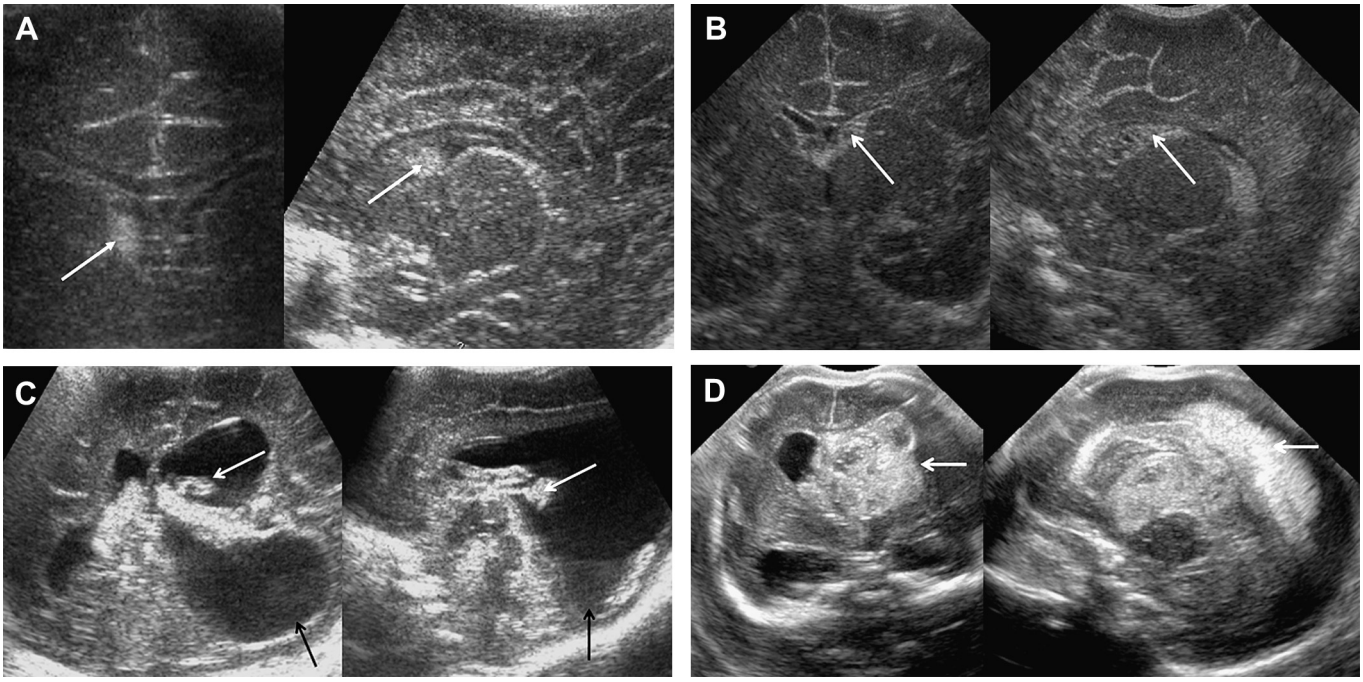

Figure 11 Neurosonographic appearance of intraventricular haemorrhage of different grades. (A) Grade I germinal matrix haemorrhage (GMH). Note the increased echogenecity of the subependymal tissue in the right caudothalamic groove (white arrows). (B) Grade II GMH. Clinically the baby presented with a rapid increase in head circumference with widened sutures. There is extension of echogenic blood clot in the frontal horn of the left lateral ventricle (white arrows). There is no intraparenchymal haemorrhage or hydrocephalus. (C) Grade III GMH. There is residual blood clot adhered to the choroid plexus (white arrows) with associate post-haemorrhagic hydrocephalus (black arrows). No intraparenchymal haemorrhage. (D) Grade III GMH with periventricular haemorrhagic infarction. The entire ventricular system is filled with echogenic blood, resulting in obstructive hydrocephalus. On the left, there is also intraparenchymal haemorrhage consistent with periventricular haemorrhagic infarction (white arrows). There is mild rightward midline shift with flattening of the sulci/gyri pattern.

approximately 50% of cases of cerebral palsy occur in individuals born prematurely.[44] Cerebral palsy occurs in up to 5% of infants born before 32 weeks and up to 19% of infants born before 28 weeks gestational age.[11] In term patients, the prevalence of HIE is estimated to be between two and four per 1000 live births,[45] of these 15% and 20% of infants die during the neonatal period, and an additional 25% develop permanent neurological disabilities.[46]

Childhood hypoxic brain injuries can present with different distributional patterns depending on various factors. These include the maturity of the brain, child's age at the time of the insult, severity of hypotension and duration of the injury. During severe hypotension, preterm and term neonates are vulnerable to hypoxic injury to the thalami, basal ganglia (figure 7) and brainstem. In addition, the dorsal brainstem and peri-rolandic cortex are typically involved in term neonates, whereas these findings are unusual in preterm neonates.[10 47] In older children, diffuse cortical injury (figure 8A) and basal ganglia lesions dominate. Characteristically the cerebellum, being less susceptible to the hypoxic ischaemic change, remains higher in

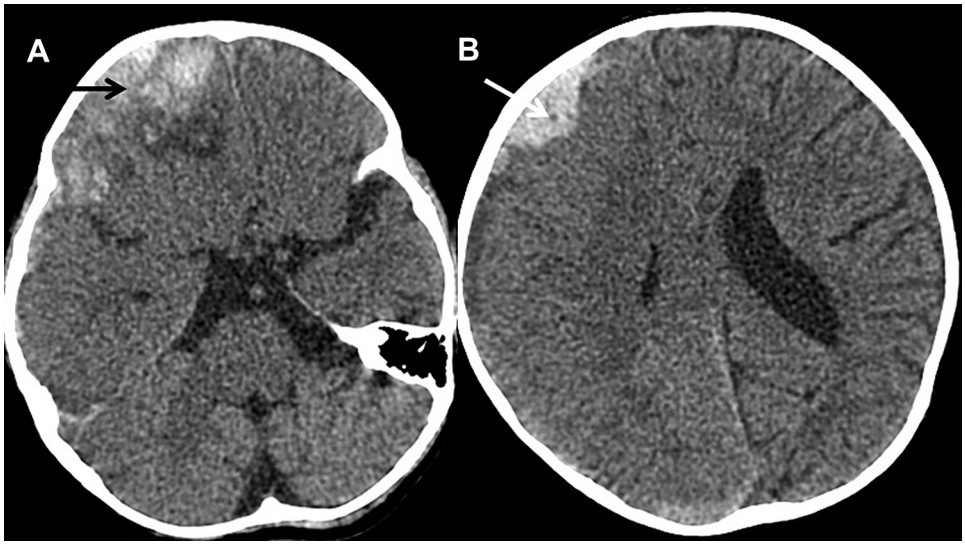

Figure 12 A 15-year-old boy presented with sudden onset of disorientation and right-sided weakness. CT brain: unenhanced images (A) showing right frontal lobe haemorrhage and perilesional white marrow oedema (black arrow) and (B) showing right epidural haematoma (white arrow). The boy later was found to have haemophilia A.

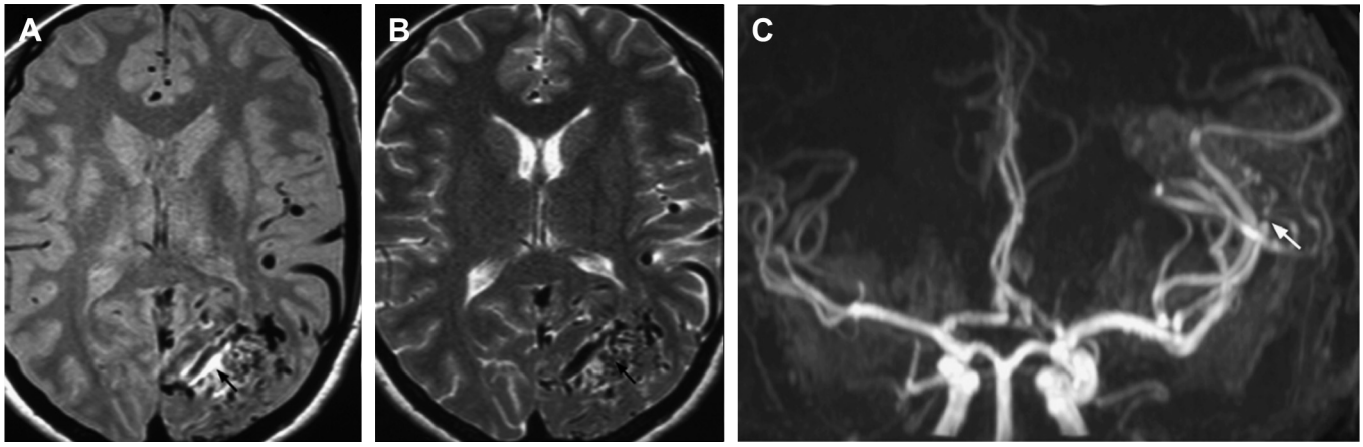

Figure 13 A 16-year-old boy presented with progressive visual loss on left side. There was a history of gradual progressive right upper and lower limb weakness. (A) Proton density image and (B) T2-weighted axial images showing left occipital infarct with bunch of serpiginous structures with flow voids (black arrow). (C) Magnetic resonance cerebral angiogram time of flight technique showing tufts of vessels arising from the left middle cerebral artery compatible with cerebral arteriovenous malformation (white arrow).

attenuation than the hypodense infarcted cerebral hemispheres on CT, producing the 'reversal sign' (figure 8B).

Cortical grey matter is more vulnerable to ischeamia when compared with white matter. The ischaemic injury to cortical neurons is known as 'cortical laminar necrosis'. Cortical laminar hyperintensity on T2-weighted and fluid-attenuated inversion recovery images is invariably seen as early as day 1 after injury, whereas hyperintensity on T1-weighted images usually occurs at least 14 days after the injury[48] (figure 8C,D). DWI may be able to detect abnormal hyperintensity in grey matter as early as less than 24 h at the early subacute phase with an adjusted window level depending on the magnetic resonance manufactures. The above imaging finding has been correlated with a poor outcome, either a permanent vegetative state or brain death.[49] Unlike profound hypotension, mild and moderate hypotension allows shunting of blood flow into the brainstem, cerebellum and basal ganglia. In preterm neonates, periventricular white matter injury prevails (figures 9 and 10), whereas term neonates and older children have parasagittal watershed injuries.[10]

Table 1 Temporal changes of haematoma on MR imaging

Stage and time from haematoma	Haemoglobin (Hb) stage	Signal intensity on T1W	Signal intensity on T2W
Hyperacute (<6 h)	Oxy-Hb	Grey	White
Acute (<6–3 days)	Deoxy-Hb	Grey	Black
Early subacute (3–7 days)	Intracellular meth-Hb	White	Black
Late subacute (1–4 weeks)	Extracellular meth-Hb	White	White
Early chronic (>4 weeks)	Extracellular meth-Hb with hemosiderin rim	White	White with black rim
Late chronic (months to years)	Hemosiderin	Black	Black

Mild to moderate asphyxia in preterm neonates can lead to intraventricular haemorrhage (IVH), the overall prevalence of which is inversely related to gestational age and weight at birth. Preterm neonates weighing less than 2000 g are approximately 25%, and in the majority of cases this bleeding

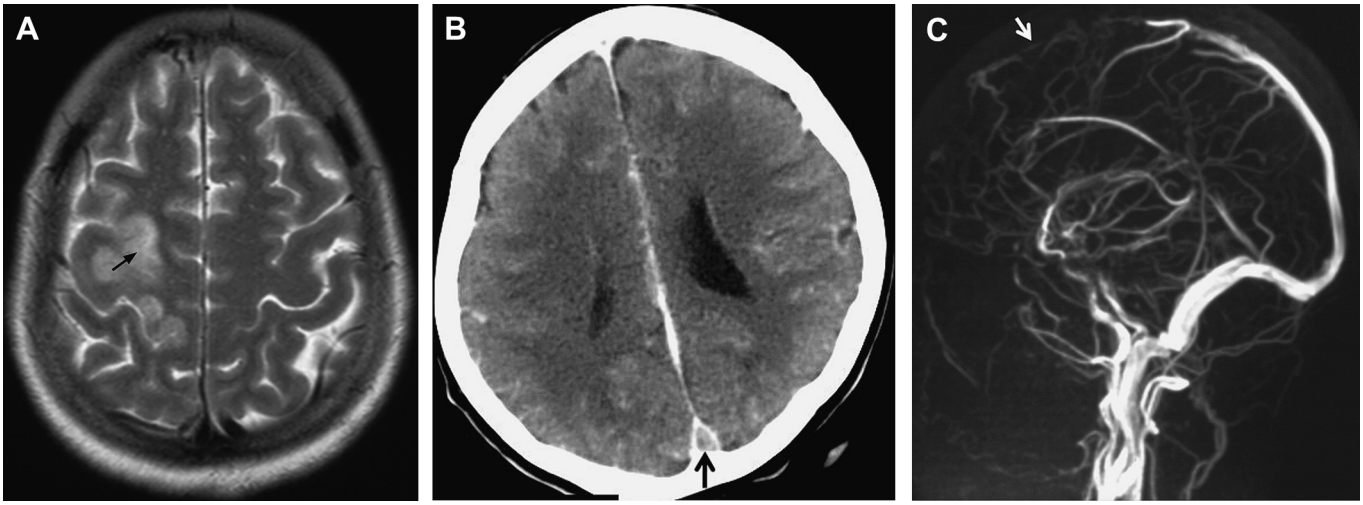

Figure 14 A 17-year-old boy presented with recurrent headache and left-sided weakness. Cranial MRI: (A) Axial T2-weighted image shows hyperintensities in the right frontal lobe (black arrow) predominantly involving the white matter. (B) Post-contrast axial image shows the empty delta sign (white arrowhead). (C) Magnetic resonance venogram using time of flight technique showing absent anterior sagittal sinus (white arrow). Features are compatible with cerebral sinovenous thrombosis.

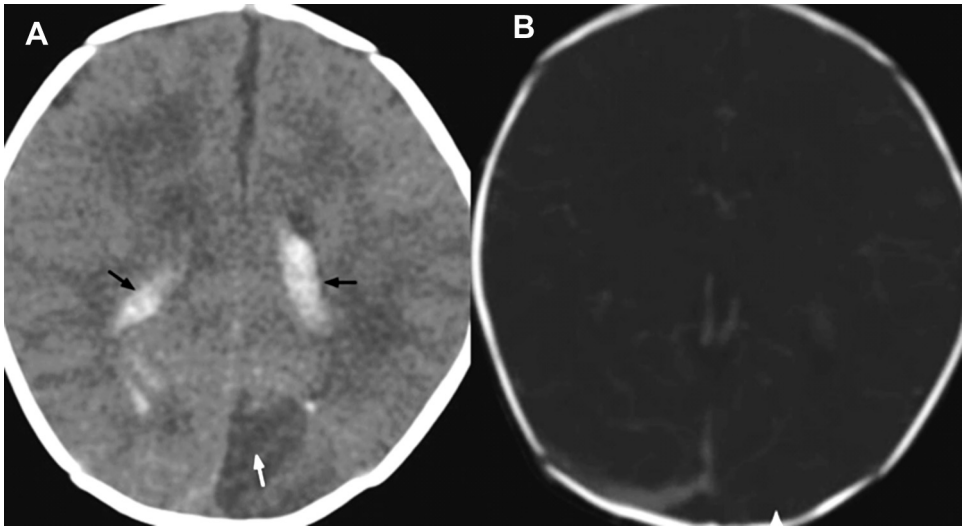

Figure 15 Day 1 child noticed to have fever soon after birth. He presented with mild respiratory distress, grunting and mild in-sucking. Neurological examination showed increasing tones over four limbs. Urgent CT: (A) Unenhanced axial CT shows left occipital infarct (white arrow) and intraventricular haemorrhages (black arrows). (B) Post-contrast image shows absent/thrombosed left transverse sinus (white arrowhead).

occurs within the first 24 h of life.[11 50 51] The majority of IVH are in turn associated with germinal matrix haemorrhages. IVH can be divided into grades I–III and grade III with periventricular haemorrhagic infarction (equivalent to the previous 'IVH grade IV').[47] The classification is based on radiological appearance rather than pathophysiological description of events leading to periventricular haemorrhage–IVH. In grade 1 haemorrhage, blood is limited to the subependymal region and/or germinal matrix (figure 11A). In grade II, there is subependymal haemorrhage with extension into the lateral ventricles without ventricular enlargement (figure 11B). In grade III, subependymal haemorrhage extends into the lateral ventricles with ventricular enlargement (figure 11C). Previously known as grade IV haemorrhage, recently termed grade III with periventricular haemorrhagic infarction (figure 11D), this condition is probably related to increased venous pressure within the terminal veins and feeders leading to periventricular haemorrhage.

Haemorrhagic stroke

Haemorrhagic stroke is rare in children. The reported incidence is approximately 1.2 per 1 000 000 children per year.[1] Traumatic head injury, non-accidental injury, bleeding disorders (haemophilia) (figure 12), arteriovenous malformations (figure 13), haemorrhagic neoplasms are some of the leading causes of haemorrhagic stroke in children.[52] As a result of faster acquisitions, CT is considered the preferred imaging investigation in these unstable patients. Depending on the stage of haematoma, MRI can detect various blood products and predict the time of onset of intracranial bleeding (table 1).[53] These stages are, however, well studied in the adult population and need some caution about the interpretation of absolute time values based on imaging appearances in the paediatric population.

In the paediatric population, the presence of SDH, particularly in the absence of a history of significant accidental trauma, should alert clinicians to the possibility of a non-accidental head injury (NAHI). SDH at multiple sites, the presence of subdural blood in the posterior interhemispheric fissure or the posterior fossa are some of the features that favour the diagnosis of NAHI over accident trauma.[46] NAHI-associated skull fractures are usually multiple, bilateral, diastatic and often cross suture lines.[44] Various types of other parenchymal injuries can be seen following NAHI, in which the most common type is generalised

Main messages

- Significant overlap is present in clinical history, presentation and neurological examination in paediatric stroke and stroke mimics posing a diagnostic challenge to physicians.
- Imaging plays an important role in the clinical decision thus tremendously affecting the outcome of patients in paediatric stroke.
- Neurosonography is the preferred imaging modality for evaluating hypoxic brain injury in neonates; however, its sensitivity is low particularly in the first week of life and thus a negative study should not be interpreted as normal.
- DWI is the mainstay of diagnosis in acute AIS detecting restricted diffusion due to cytotoxic oedema, which can be detected within minutes of onset allowing quick and reliable detection of ischaemic/infarcted areas.
- Abnormal bleeding commonly occurs in glutaric aciduria type 1 and may raise the suspicion of non-accidental injury due to the presence of SDH. However, symmetric widening of the sylvian fissures with poor operculisation giving rise to 'bat wings appearance' accompanied by an expansion of external cerebrospinal fluid spaces, frontotemporal volume loss and chronic subdural collections are classically present in glutaric aciduria type 1 and are helpful in differentiating these two conditions.
- The distribution of hypoxic brain injuries depends on the maturity of the brain, child's age at the time of the insult, severity of hypotension and duration of the injury. The changes in preterm and term 'profound' hypoxic ischaemic injury are very similar, and are centred on the basal ganglia and thalami. The difference is that at term, the periorolandic cortex and brainstem cortex can also be seen, whereas these findings are unusual preterm.
- Forty per cent of paediatric patients with venous thrombosis have venous infarction; 70% of venous infarctions are haemorrhagic.
- The presence of haemorrhagic infarct should alert the clinician to the possibility of venous stroke/thrombosis and warrants contrast-enhanced venography rather than less reliable contrast images.

Current research questions

- Is the MRI interpretation of absolute time values of intracranial haematoma based on imaging appearances applicable to the paediatric population?
- What is the best imaging protocol for paediatric stroke?

parenchymal changes caused by hypoxic–ischaemic change. Less commonly, focal lesions including axonal shearing injuries do not usually contribute to death in child abuse when compared with hypoxic–ischaemic changes.[54 55]

Venous stroke/thrombosis

Cerebral sinovenous thrombosis (CSVT) occurs in 0.41 per 100 000 live-born infants,[56] and 40% of paediatric patients with venous thrombosis have venous infarction. Seventy per cent of venous infarctions are haemorrhagic.[57] Clinically, infants most commonly present with seizures and diffuse neurological symptoms. Focal neurological signs, headache and alteration of consciousness are typical symptoms in older children. Venous infarctions involve non-arterial territories and tend to be multiple, bilateral and occur over the convexities. The presence of haemorrhagic infarct should alert the clinician to the possibility of CSVT[10] (figure 14A). The 'delta sign', a hyperdensity within the triangular superior sagittal sinus on the unenhanced study suggests the diagnosis of CVST. The 'empty delta sign' of CSVT wherein thrombus is seen as a filling defect within the posterior portion of the superior sagittal sinus (figure 14B) requires the presence of intravenous contrast, which is not always given in routine protocols for intracranial haemorrhage, or in the emergency department. A dedicated venogram instead of less focused contrast-enhanced CT is recommended in a high index of clinical suspicion[58] (figure 14C). CSVT should be suspected in infants who present with IVH (figure 15), especially when associated with unilateral thalamic haemorrhage.[59] Thirty-one per cent of term infants diagnosed with CSVT were shown to be associated with IVH.[59] The location of the secondary infarction depends on which draining veins are occluded. Superior sagittal and lateral sinuses are most frequently involved, followed by straight sinus.[56 57] Deep cerebral vein thrombosis is associated with bilateral thalamic haemorrhages.

In conclusion, this pictorial essay discusses the imaging appearances and imaging protocol in paediatric stroke. Imaging plays an important role in the clinical decision, thus tremendously affecting the outcome of patients in paediatric stroke.

Key references

- **Pavlakis SG**, Kingsley PB, Bialer MG. Stroke in children: genetic and metabolic issues. *J Child Neurol* 2000;**15**:308–15.
- **Shellhaas RA**, Smith SE, O'Tool E, *et al*. Mimics of childhood stroke: characteristics of a prospective cohort. *Pediatrics*. 2006;**118**:704–9.
- **Miyamoto O**, Auer RN. Stroke in children: the coexistence of multiple risk factors predicts poor outcome. *Neurology* 2000;**54**:362–78.
- **Beitzke D**, Simbrunner J, Riccabona M. MRI in paediatric hypoxic–ischaemic disease, metabolic disorders and malformations – a review. *Eur J Radiol* 2008;**68**:199–213.
- **Eichler F**, Krishnamoorthy K, Grant PE. Magnetic resonance imaging evaluation of possible neonatal sinovenous thrombosis. *Pediatr Neurol* 2007;**37**:317–23.

MULTIPLE CHOICE QUESTIONS

1. The first imaging technique of choice in neonates and young infants to rule out intracranial abnormality is

A. CT scan.
B. MRI.
C. Ultrasound.
D. Plain x-ray of the skull.

2. The following are the important findings regarding cerebral infarction, which should be included in imaging report except

A. Areas of haemorrhages.
B. Acute versus chronic.
C. Territory involved.
D. Mass effect.
E. Areas of calcifications.

3. The signal of an early subacute infarct on MRI would appear as

A. Decreased on ADC and increased on DWI.
B. Decreased on ADC and DWI.
C. Increased on ADC and DWI.
D. Increased on ADC and decreased DWI.

4. All are correct regarding the appearance of intraparenchymal blood on MRI except

A. Hyperacute blood (<6 h) is grey on T1-weighted and white on T2-weighted MRI.
B. Late chronic blood (months to years) has black signal on both T1-weighted and T2-weighted MRI as a resuslt of haemosiderin.
C. MRI signal in the acute phase (6–72 h) is grey on T1-weighted and black on T2-weighted MRI.
D. Late subacute blood (1–4 weeks) has black signal on both T1-weighted and T2-weighted MRI as a result of haemosiderin.

5. Regarding tuberculous meningitis, all the options are correct except

A. Most common in developing country.
B. Complications include hydrocephalus, empyema and abscess.
C. Negative imaging virtually excludes the possibility of meningitis.
D. Exudates are mainly located at basal cisterns.

Competing interests None.

Provenance and peer review Not commissioned; externally peer reviewed.

REFERENCES

1. **Fullerton HJ,** Wu YW, Zhao S, *et al*. Risk of stroke in children: ethnic and gender disparities. *Neurology* 2003;**61**:189–94.
2. **Giroud M,** Lemesle M, Gouyon JB, *et al*. Cerebrovascular disease in children under 16 years of age in the city of Dijon, France: a study of incidence and clinical features from 1985 to 1993. *J Clin Epidemiol* 1995;**48**:1343–8.
3. **Steinlin M,** Pfister I, Pavlovic J, *et al*. The first three years of the Swiss Neuropaediatric Stroke Registry (SNPSR): a population-based study of incidence, symptoms and risk factors. *Neuropediatrics* 2005;**36**:90–7.
4. **deVeber G;** Canadian Paediatric Ischemic Stroke Study Group. Canadian paediatric ischemic stroke Registry: analysis of children with arterial ischemic stroke [abstract]. *Ann Neurol* 2000;**48**:514.

5. **Lynch JK,** Hirtz DG, DeVeber G, *et al*. Report of the National Institute of Neurological Disorders and Stroke Workshop on perinatal and childhood stroke. *Pediatrics* 2002;**109**:116—23.
6. **Lynch JK,** Han CJ. Pediatric stroke: what do we know and what do we need to know? *Semin Neurol* 2005;**25**:410—23.
7. **Lee J,** Croen LA, Backstrand KH, *et al*. Maternal and infant characteristics associated with perinatal arterial stroke in the infant. *JAMA* 2005;**293**:723—9.
8. **Shellhaas RA,** Smith SE, O'Tool E, *et al*. Mimics of childhood stroke: characteristics of a prospective cohort. *Pediatrics* 2006;**118**:704—9.
9. **Hatzitolios A,** Savopoulos C, Ntaios G, *et al*. Stroke and conditions that mimic it: a protocol secures a safe early recognition. *Hippokratia* 2008;**12**:98—102.
10. **Beitzke D,** Simbrunner J, Riccabona M. MRI in paediatric hypoxic—ischemic disease, metabolic disorders and malformations — a review. *Eur J Radiol* 2008;**68**:199—213.
11. **Huang BY,** Castillo M. Hypoxic—ischemic brain injury: imaging findings from birth to adulthood. *Radiographics* 2008;**28**:417—39; quiz 617.
12. **Stark JE,** Seibert JJ. Cerebral artery Doppler ultrasonography for prediction of outcome after perinatal asphyxia. *J Ultrasound Med* 1994;**13**:595—600.
13. **Babcock DS,** Ball W Jr. Postasphyxial encephalopathy in full-term infants: ultrasound diagnosis. *Radiology* 1983;**148**:417—23.
14. **Barkovich A.** *Pediatric Neuroimaging*, 4th edn. Philadelphia, 2005.
15. **Malik GK,** Pandey M, Kumar R, *et al*. MR imaging and in vivo proton spectroscopy of the brain in neonates with hypoxic ischemic encephalopathy. *Eur J Radiol* 2002;**43**:6—13.
16. **Krishnamoorthy KS,** Soman TB, Takeoka M, *et al*. Diffusion-weighted imaging in neonatal cerebral infarction: clinical utility and follow-up. *J Child Neurol* 2000;**15**:592—602.
17. **De Vries LS,** Van der Grond J, Van Haastert IC, *et al*. Prediction of outcome in new-born infants with arterial ischaemic stroke using diffusion-weighted magnetic resonance imaging. *Neuropediatrics* 2005;**36**:12—20.
18. **Roach ES,** Golomb MR, Adams R, *et al*. Management of stroke in infants and children: a scientific statement from a Special Writing Group of the American Heart Association Stroke Council and the Council on Cardiovascular Disease in the Young. *Stroke* 2008;**39**:2644—91.
19. **Jones AC,** Daniells CE, Snell RG, *et al*. Molecular genetic and phenotypic analysis reveals differences between TSC1 and TSC2 associated familial and sporadic tuberous sclerosis. *Hum Mol Genet* 1997;**6**:2155—61.
20. **Ganesan V,** Prengler M, McShane MA, *et al*. Investigation of risk factors in children with arterial ischemic stroke. *Ann Neurol* 2003;**53**:167—73.
21. **Amlie-Lefond C,** Bernard TJ, Sebire G, *et al*. Predictors of cerebral arteriopathy in children with arterial ischemic stroke: results of the International Pediatric Stroke Study. *Circulation* 2009;**119**:1417—23.
22. **Braun KP,** Kappelle LJ, Kirkham FJ, *et al*. Diagnostic pitfalls in paediatric ischaemic stroke. *Dev Med Child Neurol* 2006;**48**:985—90.
23. **Sebire G,** Fullerton H, Riou E, *et al*. Toward the definition of cerebral arteriopathies of childhood. *Curr Opin Pediatr* 2004;**16**:617—22.
24. **Danchaivijitr N,** Cox TC, Saunders DE, *et al*. Evolution of cerebral arteriopathies in childhood arterial ischemic stroke. *Ann Neurol* 2006;**59**:620—6.
25. **Husson B,** Rodesch G, Lasjaunias P, *et al*. Magnetic resonance angiography in childhood arterial brain infarcts: a comparative study with contrast angiography. *Stroke* 2002;**33**:1280—5.
26. **Husson B,** Lasjaunias P. Radiological approach to disorders of arterial brain vessels associated with childhood arterial stroke-a comparison between MRA and contrast angiography. *Pediatr Radiol* 2004;**34**:10—15.
27. **Rollins N,** Dowling M, Booth T, *et al*. Idiopathic ischemic cerebral infarction in childhood: depiction of arterial abnormalities by MR angiography and catheter angiography. *AJNR Am J Neuroradiol* 2000;**21**:549—56.
28. **Axel L.** Blood flow effects in magnetic resonance imaging. *Magn Reson Annu* 1986:237—44.
29. **Yang JJ,** Hill MD, Morrish WF, *et al*. Comparison of pre- and postcontrast 3D time-of-flight MR angiography for the evaluation of distal intracranial branch occlusions in acute ischemic stroke. *AJNR Am J Neuroradiol* 2002;**23**:557—67.
30. **Ishimaru H,** Ochi M, Morikawa M, *et al*. Accuracy of pre- and postcontrast 3D time-of-flight MR angiography in patients with acute ischemic stroke: correlation with catheter angiography. *AJNR Am J Neuroradiol* 2007;**28**:923—6.
31. **Kuroda S,** Hashimoto N, Yoshimoto T, *et al*. Radiological findings, clinical course, and outcome in asymptomatic moyamoya disease: results of multicenter survey in Japan. *Stroke* 2007;**38**:430—5.
32. **Kuroda S,** Ishikawa T, Houkin K, *et al*. [Clinical significance of posterior cerebral artery stenosis/occlusion in moyamoya disease]. *No Shinkei Geka* 2002;**30**:1295—300.
33. **Yamada I,** Murata Y, Umehara I, *et al*. SPECT and MRI evaluations of the posterior circulation in moyamoya disease. *J Nucl Med* 1996;**37**:1613—17.
34. **Matsushima Y,** Inaba Y. The specificity of the collaterals to the brain through the study and surgical treatment of moyamoya disease. *Stroke* 1986;**17**:117—22.
35. **Arita K,** Kurisu K, Ohba S, *et al*. Endovascular treatment of basilar tip aneurysms associated with moyamoya disease. *Neuroradiology* 2003;**45**:441—4.
36. **Grabel JC,** Levine M, Hollis P, *et al*. Moyamoya-like disease associated with a lenticulostriate region aneurysm. Case report. *J Neurosurg* 1989;**70**:802—3.
37. **Katz DA,** Marks MP, Napel SA, *et al*. Circle of Willis: evaluation with spiral CT angiography, MR angiography, and conventional angiography. *Radiology* 1995;**195**:445—9.
38. **Yamada I,** Suzuki S, Matsushima Y. Moyamoya disease: comparison of assessment with MR angiography and MR imaging versus conventional angiography. *Radiology* 1995;**196**:211—18.
39. **Barkovich AJ,** Good WV, Koch TK, *et al*. Mitochondrial disorders: analysis of their clinical and imaging characteristics. *AJNR Am J Neuroradio* 1993;**14**:1119—37.
40. **Pavlakis SG,** Phillips PC, DiMauro S, *et al*. Mitochondrial myopathy, encephalopathy, lactic acidosis, and strokelike episodes: a distinctive clinical syndrome. *Ann Neurol* 1984;**16**:481—8.
41. **Kim IO,** Kim JH, Kim WS, *et al*. Mitochondrial myopathy-encephalopathy-lactic acidosis and strokelike episodes (MELAS) syndrome: CT and MR findings in seven children. *AJR Am J Roentgenol* 1996;**166**:641—5.
42. **Castillo M,** Kwock L, Green C. MELAS syndrome: imaging and proton MR spectroscopic findings. *AJNR Am J Neuroradiol* 1995;**16**:233—9.
43. **Brismar J,** Ozand PT. CT and MR of the brain in glutaric acidemia type I: a review of 59 published cases and a report of 5 new patients. *AJNR Am J Neuroradiol* 1995;**16**:675—83.
44. **Meservy CJ,** Towbin R, McLaurin RL, *et al*. Radiographic characteristics of skull fractures resulting from child abuse. *AJR Am J Roentgenol* 1987l;**149**:173—5.
45. **Chao CP,** Zaleski CG, Patton AC. Neonatal hypoxic—ischemic encephalopathy: multimodality imaging findings. *Radiographics* 2006;**26**(Suppl 1):S159—72.
46. **Stoodley N.** Neuroimaging in non-accidental head injury: if, when, why and how. *Clin Radiol* 2005;**60**:22—30.
47. **Barkovich AJ,** Sargent SK. Profound asphyxia in the premature infant: imaging findings. *AJNR Am J Neuroradiol* 1995;**16**:1837—46.
48. **Siskas N,** Lefkopoulos A, Ioannidis I, *et al*. Cortical laminar necrosis in brain infarcts: serial MRI. *Neuroradiology* 2003;**45**:283—8.
49. **McKinney AM,** Teksam M, Felice R, *et al*. Diffusion-weighted imaging in the setting of diffuse cortical laminar necrosis and hypoxic—ischemic encephalopathy. *AJNR Am J Neuroradiol* 2004;**25**:1659—65.
50. **Volpe JJ.** Intraventricular hemorrhage in the premature infant — current concepts. Part I. *Ann Neurol* 1989;**25**:3—11.
51. **Paneth N,** Pinto-Martin J, Gardiner J, *et al*. Incidence and timing of germinal matrix/intraventricular hemorrhage in low birth weight infants. *Am J Epidemiol* 1993;**137**:1167—76.
52. **Al-Jarallah A,** Al-Rifai MT, Riela AR, *et al*. Nontraumatic brain hemorrhage in children: etiology and presentation. *J Child Neurol* 2000;**15**:284—9.
53. **Parmar H,** Trobe JD. A "first cut" at interpreting brain MRI signal intensities: what's white, what's black, and what's gray. *J Neuroophthalmol* 2010;**30**:91—3.
54. **Geddes JF,** Vowles GH, Hackshaw AK, *et al*. Neuropathology of inflicted head injury in children. II. Microscopic brain injury in infants. *Brain* 2001;**124**:1299—306.
55. **Geddes JF,** Hackshaw AK, Vowles GH, *et al*. Neuropathology of inflicted head injury in children. I. Patterns of brain damage. *Brain* 2001;**124**:1290—8.
56. **deVeber G,** Andrew M, Adams C, *et al*. Cerebral sinovenous thrombosis in children. *N Engl J Med* 2001;**345**:417—23.
57. **Wasay M,** Dai AI, Ansari M, *et al*. Cerebral venous sinus thrombosis in children: a multicenter cohort from the United States. *J Child Neurol* 2008;**23**:26—31.
58. **Eichler F,** Krishnamoorthy K, Grant PE. Magnetic resonance imaging evaluation of possible neonatal sinovenous thrombosis. *Pediatr Neurol* 2007;**37**:317—23.
59. **Wu YW,** Miller SP, Chin K, *et al*. Multiple risk factors in neonatal sinovenous thrombosis. *Neurology* 2002;**59**:438—40.

ANSWERS

1. Correct answer: (C). Ultrasound is radiation free, can be done at the bedside. It can also be performed quickly without any need for sedation.
2. Correct answer: (E). Remaining four are the most important findings deciding plan of management in practice.
3. Correct answer: (A).
4. Correct answer: (D). Late subacute blood (1—4 weeks) is mainly due to extracellular meth-Hb, which signal appears white on both T1-weighted and T2-weighted MRI.
5. Correct answer: (C). Imaging is mainly to look for complications and may be entirely normal at early stages.

Imaging in children presenting with acute neurological deficit: stroke

Darshana D Rasalkar and Winnie C W Chu

Postgrad Med J 2012 88: 649-660 originally published online April 13, 2012
doi: 10.1136/postgradmedj-2011-130087